Chronology of the Palmer Deep site, Antarctic Peninsula: a Holocene palaeoenvironmental reference for the circum-Antarctic

E. Domack,¹ A. Leventer,² R. Dunbar,³ F. Taylor,¹ S. Brachfeld,⁴ C. Sjunneskog⁵ and ODP Leg 178 Scientific Party

(¹Department of Geology, Hamilton College, Clinton, New York 13323, USA; ²Department of Geology, Colgate University, Hamilton, New York 13346, USA; ³Department of Geological and Environmental Sciences, Stanford University, Stanford, California 94305, USA; ⁴Institute for Rock Magnetism, University of Minnesota, Minneapolis, Minnesota 55455, USA; ⁵Institute of Earth Sciences, Uppsala University, Uppsala S-752 36, Sweden)

Received 30 February 2000; revised manuscript accepted 13 July 2000



Abstract: Palmer Deep sediment cores are used to produce the first high-resolution, continuous late Pleistocene to Holocene time-series from the Antarctic marine system. The sedimentary record is dated using accelerator mass spectrometer radiocarbon methods on acid insoluble organic matter and foraminiferal calcite. Fifty-four radiocarbon analyses are utilized in the dating which provides a calibrated timescale back to 13 ka BP. Reliability of resultant ages on organic matter is assured because duplicates produce a standard deviation from the surface age of less than laboratory error (i.e., ±50 years). In addition, surface organic matter ages at the site are in excellent agreement with living calcite ages at the accepted reservoir age of ~1260 years for the Antarctic Peninsula. Spectral analyses of the magnetic susceptibility record against the age model reveal unusually strong periodicity in the 400, ~200 and 50–70 year frequency bands, similar to other high-resolution records from the Holocene but, so far, unique for the circum-Antarctic. Here we show that comparison to icecore records of specific climatic events (e.g., the 'Little Ice Age', Neoglacial, Hypsithermal, and the Bølling/Allerød to Younger Dryas transition) provides improved focus upon the relative timing of atmosphere/ocean changes between the northern and southern high latitudes.

Key words: chronology, spectral analysis, periodicity, Palmer Deep, Antarctic Peninsula, Holocene, radiocarbon, sedimentology.

Introduction

The Antarctic Peninsula region encompasses one of the most dynamic climate systems on Earth. Here ecologic and cryospheric systems respond rapidly to the pulse of climate change (Smith *et al.*, 1999), of which the most recent is a 40 year long warming trend unprecedented in the last 500 years (Thompson *et al.*, 1994). Palaeoceanographic changes can also be documented from the region such as those related to global-scale processes (Domack and Mayewski, 1999). For instance, deep waters of North Atlantic and Antarctic origin express themselves by the presence or absence of Circum-Polar Deep Water across the continental shelf, which is generally believed to represent the distal reach of

NADW. Short-term fluctuations of these water masses may hold the key to understanding climate oscillations of the late Holocene (Broecker *et al.*, 1999).

In order to understand the natural variability of the region's climate and ocean systems we need a reliable chronology for marine sediment cores. Excellent marine sediment cores are now available as obtained by the Ocean Drilling Program (Leg 178) (Barker *et al.*, 1999), cruise 98–02 of the RV *Laurence M. Gould* in March 1998 (Domack and Reynolds, 2000), and cruise 99–03 of the RV *Nathaniel B. Palmer*. Herein we examine cores obtained from the bathyal depths of the Palmer Deep, a prominent depression on the inner continental shelf of the western Antarctic Peninsula (Figure 1, 64° 51.71′ S, 64° 12.47′ W) (Kirby *et al.*,

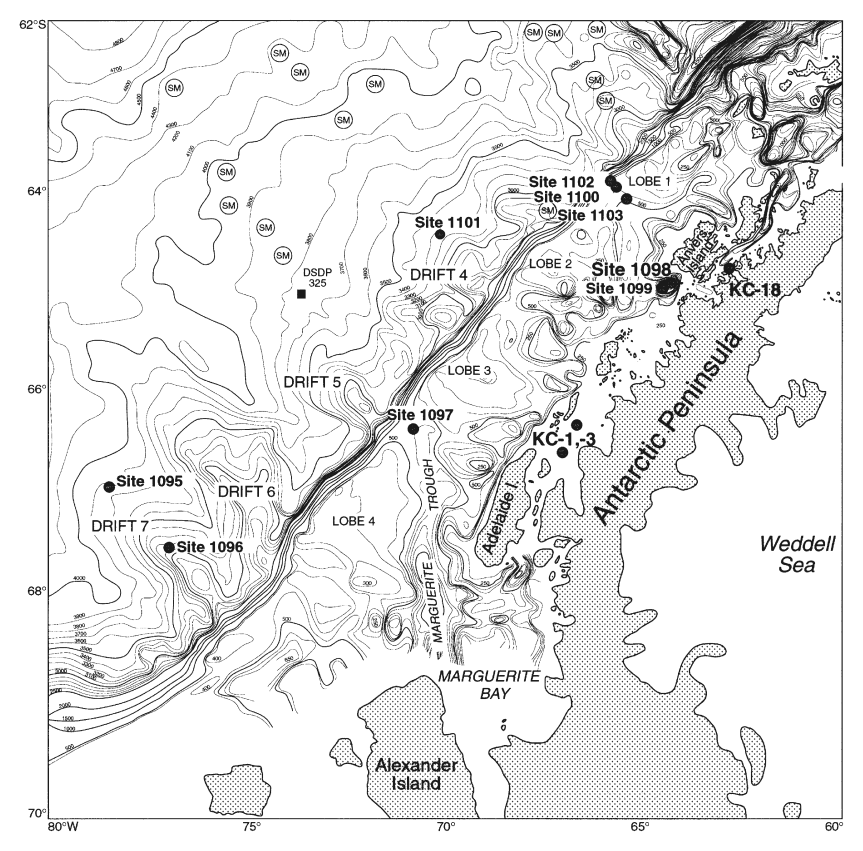


Figure 1 Location of the Palmer Deep Site 1098 and other drill sites occupied during Ocean Drilling Program Leg 178 on the Antarctic Peninsula continental margin and shelf. Location of gravity cores mentioned in text is also shown. Bathymetric contours are after Rebesco *et al.*, (1998) and are every 50 m on the shelf and every 100 m on the rise and slope. Seamounts are indicated (SM) as are the locations of hemipelagic sediment drifts (rise and slope) and glacigenic sediment lobes (middle to outer shelf).

1998). Over 50 m of section was recovered in three holes at site 1098 via advanced piston coring. The sediments consist of structureless to laminated diatom ooze/mud, rhythmically interbedded diatom ooze and pebbly mud and muddy diamicton. The latter two units comprise a deglacial phase, from subglacial (till) to proximal glacial marine sedimentation. Three thin turbidites interrupt the stratigraphy in the lower third of the section. Rapid deposition (~2 mm yr⁻¹) (Leventer *et al.*, 1996) from locally high productivity and basinal sediment focusing, along with isolation from iceberg turbation and limited glacial marine (siliciclastic/meltwater) sedimentation, provide an ideal setting from which to acquire reliable radiocarbon ages on phytoplankton organic matter and foraminiferal calcite.

Methods

Radiocarbon analyses

Modern surface samples

Surface samples were collected at the sediment water interface from a series of multicores and kasten cores that were collected in the vicinity of the Palmer Deep (Figure 1; Table 2). Duplicate radiocarbon analyses on these organic matter samples demonstrate variation from the mean value that is less than the routine laboratory (counting) error of ± 40 to 50 years. These results are significantly better than those experiments completed on surface sediments in the Ross Sea, where duplicate analyses provided errors of ± 200 years or more (Andrews et~al., 1999). Hence the Palmer Deep region is a better environment in which to utilize organic matter fractions for $^{14}{\rm C}$ analysis because of more rapid accumulation, limited detrital kerogen and more restricted benthic mixing (when compared to the Ross Sea).

Holocene intervals

Cores were opened aboard ship and samples were taken and dried immediately at 106°C for 24 hours in order to minimize secondary carbon alteration with atmospheric CO₂ via bacterial assimilation or degradation (fermentation). Samples were then processed in 2N HCl for 24 hours to remove acid soluble components, decanted, washed to neutrality, and then sent to the University of Arizona Accelerator Mass Spectrometer (AMS) laboratory for ¹⁴C analyses (see Table 1). We are confident in the total organic carbon (TOC) ages because the total organic carbon contents of all our samples are in excess of 0.7% (most have TOC greater than 1.0%) and, more importantly, we demonstrate excellent agreement between the TOC ages and selected foraminifera calcite ages (Table 1). Reworking of organic matter influences resultant ages most readily in organically lean sediments (Stuiver *et al.*, 1998).

Late-Pleistocene intervals

In providing calibrated ages for the lower intervals of Site 1098 cores we realize that there may be errors in our assumption of a near-modern reservoir correction because of the variability of δ^{14} C during the Lateglacial time (Stuiver *et al.*, 1998). We suggest therefore, that the age model for the lower interval be used with some caution until more systematic studies are done on similar and/or replicate time-series. Since CALIB 98 automatically assigns a reservoir correction of 402 years, we selected a ΔR of 830 yrs (Table 1). Together these two corrections in the calibration routine accommodate our accepted reservoir age of 1230 years on living marine organisms and surface sediments. A best-fit line for the set of ages (between turbidites 1 and 2 and 2 and 3) was then calculated. The only caveat is that in calculating a sedimentation rate for the section between turbidites 1 and 2 we also set the age at the base of turbidite 1 at 8750 cal. BP. This

Table 1 Uncorrected reservoir corrected and calibrated radiocarbon dates

Lab no. #	Core sample*	Carbon source**	Sample interval (mbsf)	mcd	Uncorrected age (BP)	± (yrs)	Corrected age (BP) R(t) = 1230	± (yrs)	Calibrated age (cal. BP) $\Delta R = 830 \pm 40$	TOC‡ (%)	θ^{13} C
AA29169	LMG98 KC1	POC	0.00-0.02	0.00	1265	40	33	40	0	1.360	-24.700
AA29168	LMG98 KC1	POC	0.30-0.34	0.32	1200	40	-32	40	0	0.975	-24.898
AA29123	1098C	POC	1.38-1.40	1.28	2200	50	970	50	920	1.230	-24.893
AA13980	PD92-30	POC	0.00-0.02	1.36	2260	55	1030	55	960	0.98	na
AA12706	PD92-30	F	1.52-1.56	2.70	2615	70	1380	70	1310	1.15	na
AA29124	1098C	POC	3.15-3.17	3.05	2480	45	1250	45	1220	1.590	-21.930
AA12707	PD92-30	F	3.12-3.16	4.36	3095	60	1860	60	1870	0.97	na
AA12708	PD92-30	F	3.92-3.96	5.10	3235	60	2000	60	2030	0.99	na
AA12376	PD92-30	POC	5.00-5.02	6.30	4145	50	2910	50	3160	na	na
AA17377	PD92-30	POC	5.90-5.92	7.28	4360	40	3130	40	3400	0.88	na
AA29125	1098C	POC	7.82–7.84	7.72	4400	45	3170	45	3450	1.110	-23.974
AA13981	PD92-30	POC	6.48-6.50	7.84	4615	80	3380	80	3700	1.03	na
AA13982	PD92-30	POC	8.09-8.11	9.68	5480	60	4250	60	4840	na	na
AA29126	1098C	POC	10.53–10.55	10.19	4865	60	3630	60	4060	1.760	-21.035
AA13983	PD92-30	POC	8.78-8.80	10.32	5130	65	3900	65	4410	na	na
AA29127	1098C	POC	11.13–11.15	10.79	5010	60	3780	60	4250	1.480	-22.260
AA29128	1098C	POC	11.88–11.90	11.54	5215	65	3980	65	4520	1.470	-22.262
AA29129	1098C	POC	12.13–12.15	11.79	5380	60	4150	60	4790	1.510	-23.537
AA29130	1098C	POC	12.86–12.88	12.52	5285	60	4050	60	4610	1.560	-20.432
AA29131	1098C	POC	14.30–14.32	13.96	5785	55	4550	55	5290	1.550	-23.344
AA29132	1098C	POC	15.75–15.77	15.41	6270	55	5040	55	5840	1.330	-23.667
AA29133	1098C	POC	16.80–16.82	16.46	6435	60	5200	60	5980	1.700	-21.986
AA29134	1098C	POC	17.21–17.23	16.87	6465	55	5230	55	5990	1.580	-22.322
AA29135	1098C	POC	18.16–18.18	17.82	7005	55	5770	55	6620	1.260	-23.753
AA29136	1098C	POC	19.55–19.57	20.17	7735	60	6500	60	7420	1.460	-22.998
AA29137	1098C	POC	20.20–20.22	20.82	8130	60	6900	60	7740	1.360	-23.233
AA29138	1098C	POC	21.33–21.35	21.95	8370	60	7140	60	7970	1.460	-23.705
AA29139 AA29140	1098C 1098C	POC POC	22.92–22.94 23.59–23.61	23.54 24.21	8825 8855	70 65	7590 7620	70 65	8420 8450	1.210 1.260	-23.993 -23.993
AA29140	1098C	POC	23.39-23.01	24.21	8833	0.3	7620	0.3	8430	1.200	-23.993
OS-24750	1098C	POC	28.69-28.71	31.12	9280	50	8050	50	8940	na	-24.17
AA29141	1098C	POC	28.77–28.79	31.19	9265	65	8030	65	8930	1.060	-24.906
AA29142	1098C	POC	29.42–29.44	31.84	9475	65	8240	65	9040	0.970	-24.541
OS-24751	1098C	POC	29.95–29.97	32.38	9860	95	8630	95	9770, 9720, 9630	na	-24.34
OS-24752	1098C	POC	32.59–32.61	35.02	10350	55	9120	55	10280	na	-22.76
OS-24753	1098C	POC	32.89–32.91	35.32	10850	55	9620	55	11050, 10990, 10830	na o zoo	-24.20
AA29143	1098C	POC	33.16–33.18	35.58	10365	70	9130	70	10280	0.798	-24.249
LL-57121	1098B	F	33.50–33.51	35.69	9890	50	8660	50	10290	na	0
OS-24711	1098C	POC	33.75–33.77	36.20	10500	65	9270	65	10310	na o zo i	-23.31
AA29144	1098C	POC	35.04–35.06	37.46	10585	70	9360	70	10550, 10490, 10340	0.701	-24.249
OS-24754	1098C	POC	35.87–35.89	38.25	10700	65	9470	65	10620	na	-23.460 0
LL-57122	1098B	F F	37.05–37.06	38.80	10410	80	9180	80	11090, 10980, 10840	na	_
Ua-14999	1098C		39.97–40.02	41.53	11295	90	10070	90	11600, 11530, 11370	na 0.007	-14.4
AA29145 OS-24755	1098C 1098C	POC POC	39.50–39.52 40.03–40.05	43.89 44.43	11410 11850	70 55	10180 10620	70 55	11671 12270, 12460, 12430	0.997	-21.930 -22.01
OS-24755 AA29146	1098C 1098C	POC	40.03-40.05	44.43	11850	55 75	10620		12270, 12460, 12430	na 1.600	-22.01 -20.802
	1098C 1098C							75 60			
OS-24756	1098C 1098C	POC	40.45–40.47	44.85	11550	60 55	10320	60	11940, 11800, 11760	na	-20.98 20.43
OS-24757		POC	41.24-41.26	45.64	11300	55	10070	55	11600, 11530, 11370	na	-20.43
OS-24758	1098C	POC	41.92–41.94	46.32	12250	60 80	11020	60	12970	na o ose	-21.76
AA29147	1098C 1098A	POC F	41.95–41.97	46.34 47.46	12015 10565	80 105	10780 9340	80 105	12830, 12700, 12690 10322	0.956	-22.315 -7.3
Ua-14998	1098A	Г	44.27–44.32	47.40	10303	103	9340	103	10322	na	-1.5

^{*}LMG98-2 = Laurence M. Gould cruise 1998-02, PD92 = Polar Duke cruise 1992-02, ODP = Ocean Drilling Program Leg 178 Site 1098 (A, B, C) (JOIDES Resolution).

#AA = University of Arizona Accelerator Lab, OS = National Ocean Sciences Accelerator Lab (WHOI), LL = Center for Accelerator Mass Spectrometry (Lawrence Livermore National Laboratory), Ua = Uppsala University Accelerator Lab.

Table 2 Uncorrected radiocarbon dates for surface samples collected on NBP99-03

Lab no.	Core	Carbon	Depth	Uncorrected age	±	TOC (%)	θ ¹³ C
AA34635 AA34642 AA34644	KC-1 KC-3 KC18-B KC18-C	POC POC POC POC	0–2 cm 0–2 cm 0–2 cm 0–2 cm	1830 1820 1445 1450	40 45 55 40	0.594 0.800 na 1.02	-22.900 -23.100 -23.400 -23.400

NBP99-03 = Nathaniel B. Palmer cruise 1999-03.

age is close to the age calculated for the top of turbidite 1 based on the age model for the upper 25 m of the core.

Within the lower 30 m of the core we also incorporated analyses from three other laboratories and in so doing assume uniformity of inter-laboratory errors. This assumption may not be accurate and needs further evaluation between the National Ocean Sciences Accelerator Laboratory at Woods Hole, the Lawrence Livermore National Laboratory and the Uppsala University Accelerator Laboratory in Sweden.

Spectral analyses

Spectral analysis of the magnetic susceptibility (MS) data was done with the Singular Spectrum Analysis Toolkit SSA-MTM

^{**}POC = acid insoluble organic carbon, F = benthic foraminifera.

[†]Uncorrected ages rounded to the nearest half-decade, reservoir and calibrated ages rounded to the nearest decade. Where more than one calibrated age is given all possible intercept ages are provided for \pm one sigma. All uncorrected ages are adjusted for the measured δ^{13} C except those from LL, where a value of 0 is assumed for foraminiferal calcite.

[‡]TOC = % total organic carbon.

(version 3) available from http://www.atmos.ucla.edu/tcd/ssa/. The data were run through the ARAND program TIMER (from Philip J. Howell at Brown University) to yield an equal time-step of seven years. The Multi-Taper method was used because of better estimation of confidence to place on individual peaks, identification of harmonics, and less spectral leakage out of peaks.

Results

Radiocarbon dates

The results of 51 radiocarbon analyses on the Palmer Deep sediments are listed in Table 1. Ages are reported as uncorrected, reservoir corrected and age calibrated (cal. BP). Their downcore trend is illustrated in Figures 1 and 2. The depth scale is provided for metres below the seafloor (mbsf) in each hole at site 1098 and as a composite depth scale determined by Acton et al. (2000). Although temporal variations in the Antarctic marine reservoir of ∂^{14} C are as yet unknown, we assume a local correction that accounts for both the reservoir and reworking of particulate organic matter at the site of deposition. This method is consistent with the procedures established recently for the Antarctic Peninsula (Domack and McClennen, 1996) and Ross Sea (Domack et al., 1999; Andrews et al., 1999). Yet, the Palmer Deep marine sequence is exceptional. This is because surface ages on organic matter, 1265 ± 40 BP (AA29169) and 1200 ± 40 BP (AA29168)

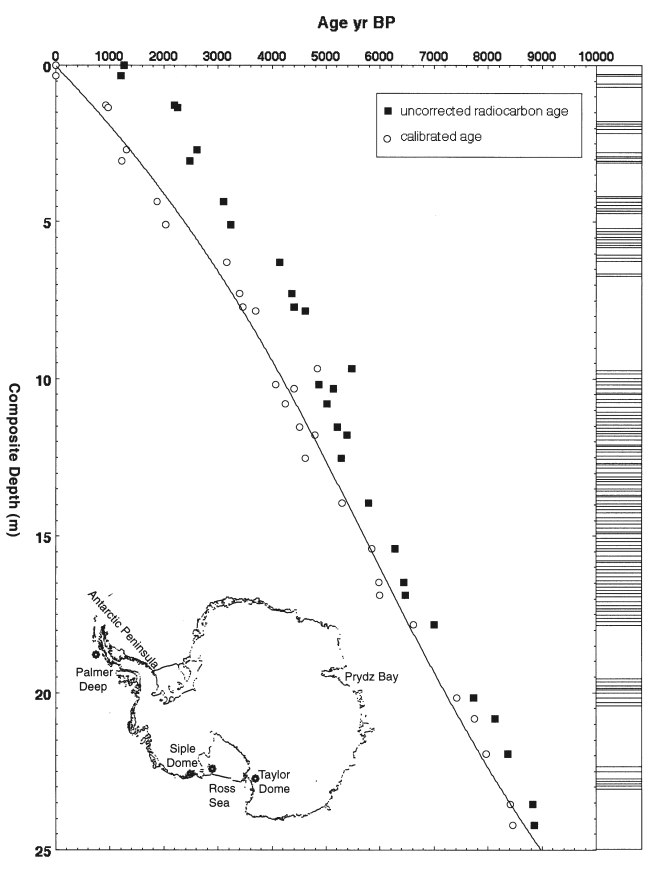


Figure 2 Depth versus radiocarbon age for the upper 25 m at site 1098 of ODP Leg 178 in the Palmer Deep, Antarctica. The depth scale (in metres composite depth) is a composite of three holes (1098/A-C) and is cross-correlated with kasten core LMG98-01 and piston core PD92-30 (see Table 1 for details). The ages are given as uncorrected radiocarbon ages and calibrated ages following the most recent routine for calibration of radiocarbon ages (Stuiver et al., 1998). Laminated intervals are illustrated within the core log. A third-order polynomial is regressed against the calibrated ages to provide a chronology model. Insert shows location of the Palmer Deep deposystem, and Taylor Dome and Siple Dome ice cores, in the regional framework of Antarctica.

(Table 1), are equivalent, or less than, ages of biogenic calcite in living marine invertebrates (1260 \pm 60 BP and 1240 \pm 80 BP) from the same region (Domack, 1992). Such ages are accepted as representing the reservoir age of shelf waters in the Antarctic (Berkman and Forman, 1996; Gordon and Harkness, 1992).

Age model calibration

The progression of ages represents near-continuous sedimentation for the Holocene epoch which extends into the latest Pleistocene (Figures 2 and 3), thereby providing an Antarctic marine radiocarbon stratigraphy of unequalled temporal resolution for the last 13000 cal. BP. The time-series is divided into two intervals: the upper 25 m composite depth (0-9000 cal. BP) and the lower 25 m (~9000-13000 cal. BP). This is done because three turbidites interrupt the stratigraphy in the lower part of the core. The upper 25 m is regressed using a third-order polynomial:

$$y = -16.476 + 556.18x - 17.379x^2 + 0.38109x^3$$
 (1)

where y = age(yr) and x = depth(m), which provides a better fit $(R^2 = 0.990)$ to the data than a simple linear trend $(R^2 = 0.950)$ and is more consistent with the actual stratigraphy (Figure 2).

The basic trend of equation (1) is that sedimentation rates vary, from 0.17 cm yr⁻¹ in the late Holocene to 0.24-0.34 cm yr⁻¹ in the mid-Holocene and 0.25 cm yr⁻¹ in the early Holocene. This

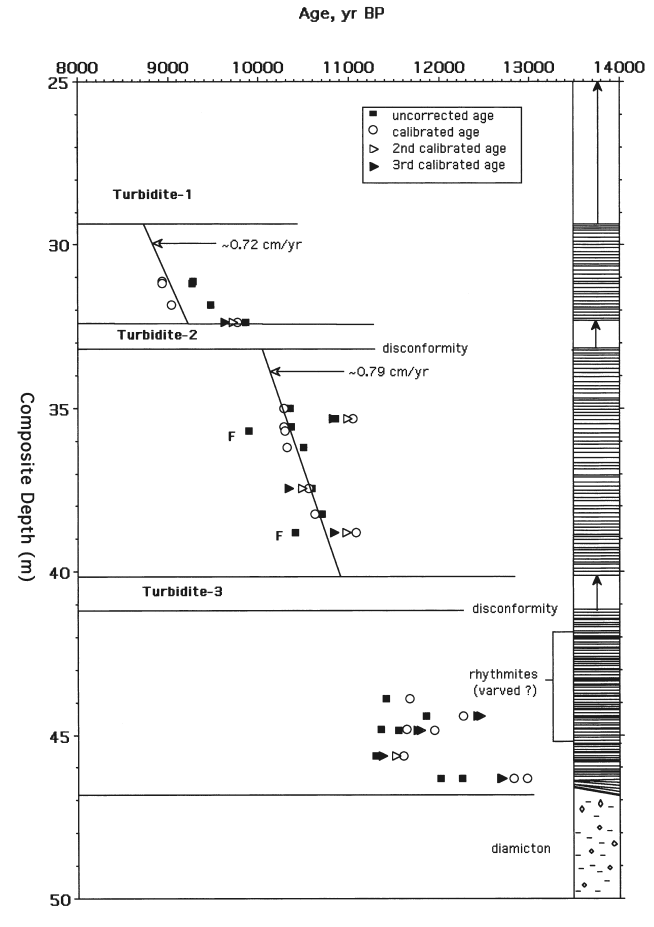


Figure 3 Depth versus radiocarbon age for the lower 25 m at site 1098. The depth scale is a continuation of that illustrated in Figure 1. Data are given as uncorrected radiocarbon ages and calibrated ages using a standard 1230-year 'reservoir correction'. A variety of calibrated ages result from a single corrected age because of the variability of $\partial^{14}C$ during the glacial to interglacial transition (Stuiver et al., 1998). Note the erosional disconformities at the base of turbidites 2 and 3. Core stratigraphy is illustrated in the core log, with a basal diamicton overlain by draped (inclined) laminated intervals and turbidites (vertical arrows). Horizontal laminations begin at ~32 m. Linear sedimentation rates are also provided.

provides a resolution of 5-3 years cm⁻¹. With few exceptions, differences between equation (1) and the actual data points are all close to the laboratory errors compounded by calibration (Stuiver et al., 1998) (Figure 4). The differences are also within ± 200 years determined for replication of organic matter ages in siliceous muds/oozes of the Ross Sea, where sedimentation rates are lower (Andrews et al., 1999). The only outlier in the data set is an anomalously old, uncorrected age of 5480 \pm 60 BP (AA13982) at 9.68 m. The calibrated age is \sim 750 years older than the age model (Fig. 4). Short-term variations in surface mixing, upwelling of shelf deep waters (such as Circumpolar Deep Water (CDW)), and short-term variations in sedimentation rate and/or bioturbation depth may contribute to this effect.

Below 25 m, the age model is developed with three sets of corrected ages each separated from each other by a mud turbidite interval (Figure 3; see Methods). The first two intervals, between composite depths of 25 and 40 m, show a consistent increase in age versus depth while the lowermost interval demonstrates no consistency in age versus depth, suggesting very rapid sedimentation. The scatter in ages in the upper two intervals is probably a product of:

(1) differences between calcite (foraminifera) and organic matter

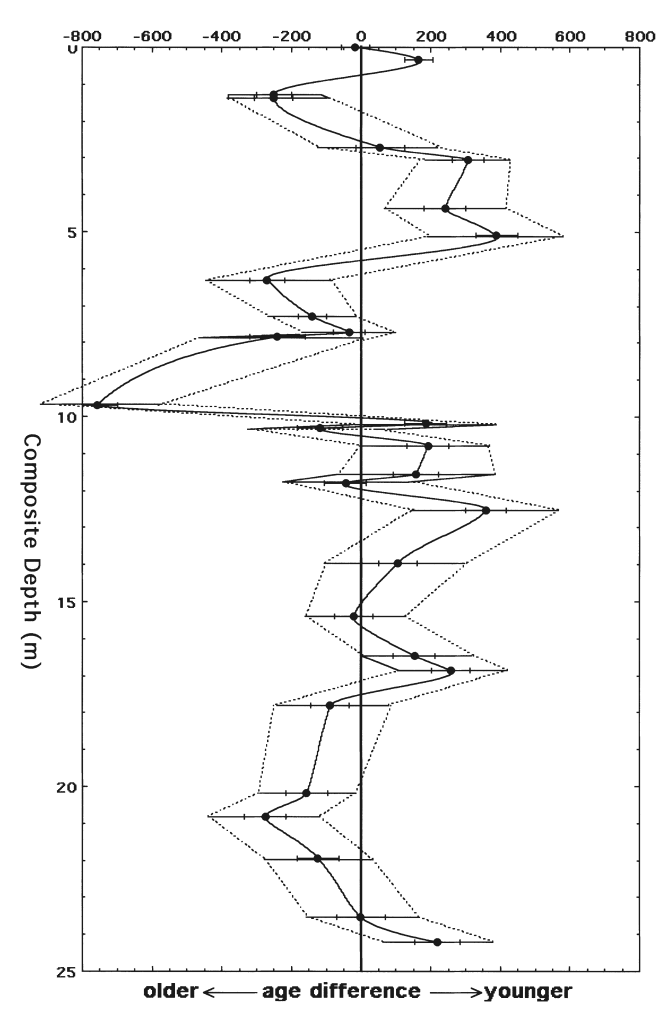


Figure 4 Variation of calibrated ages against the chronological model in Figure 1. Residuals are plotted as deviations from the model in calendar years with ages older than the model to the left and younger than the model to the right. Error bars indicate laboratory errors for each data point; dashed lines indicate the calculated two-sigma for the calibrated ages. Some variations from the model ages are believed to be significant and most likely result from short-term (millennial-scale) changes in accumulation rate and/or local reservoir variability not accounted for in the accumulation model.

- ages of between 400 and 500 years, with the forams being younger than depth equivalent organic matter ages;
- (2) the variance of calibrated ages for a single corrected age using the CALIB-98 program (Stuiver et al., 1998); and
- (3) some discrepancy among the various laboratories that produced ages in this interval.

Production of true calibrated ages for this time-frame is also difficult since it is known that the lower intervals were deposited in a shelf environment that had reduced CDW influence (Barker et al., 1999). The time interval (~10000-13000 cal. BP) is known to have had less North Atlantic Deep Water production and, hence, less antiquity (50-80%) for the radiocarbon reservoir in the Southern Ocean (Hughen et al., 1998). Hence, for Antarctic shelf waters it might reasonably be assumed that a reduction in the reservoir effect is likely, although its magnitude is uncertain

Between turbidites 1 and 2 (Figure 3) a sedimentation rate of 0.72 cm yr⁻¹ was determined, greater than sediments overlying turbidite 1. The base of turbidite 1 is marked by sandy diatomaceous mud that grades upward into diatom ooze, indicating the likelihood that turbidite deposition was not preceded by significant erosion. The age model also indicates no loss of section at the base of turbidite 1. In contrast, the age model developed between 33 and 40 m depth shows a loss of almost 1000 years at the base of turbidite 2 (Figure 3), which is marked by a coarse sand and gravel layer. It is likely that erosion occurred at the time of turbidity flow. Rates of sedimentation increase in this section to 0.8 cm yr⁻¹. The anomalous age at 32.28 m depth appears to be related to some imprecision in the Uppsala University Laboratory, as it is out of line with three other dates in this interval.

A reasonable chronology for the section of core below the third turbidite (below 40 m depth) was difficult to develop. Overall the ages are significantly older than the overlying interval, suggesting postglacial deposition about 13000 yr BP. The post-diamicton sediments consist of a ~5 m section of rhythmically laminated sediments that are probably varved (McAndrews et al., 2000).

Initial analysis of ~176 light and dark couplets indicates a regular alternation between spring bloom diatom species and lower productivity assemblages associated with concentrations of icerafted debris (Leventer, 1998; McAndrews et al., 2000; Katz, 2000). Therefore, the lack of progression of ages down section in this interval probably represents temporal variations that are not resolved by the radiocarbon method, given the other problems in radiocarbon systems in glacier-proximal settings (changing reservoir effects, vital effects between interannual phytoplankton blooms; Domack et al., 1999). This section of the core is marked by high total organic carbon contents, suggesting little contamination by particulate (detrital) carbon, but the carbon is isotopically enriched in ¹³C (Table 1), suggesting high primary production and possible CO₂ draw-down effects in the surface waters.

Discussion

Palaeoenvironmental succession

Although a complete suite of palaeoenvironmental proxies has yet to be integrated for this site, we can utilize the chronological constraints coupled with magnetic susceptibility (MS), mass accumulation rate (MAR) and ice-rafted debris (IRD) in order to propose five prominent palaeoenvironmental intervals (Figure 5):

- (1) the Neoglacial, beginning at 3360 cal. BP and including the 'Little Ice Age' starting at ~700 cal. BP and ending ~100 cal. BP;
- (2) a mid-Holocene climatic optimum (Hypsithermal) from 9070 cal. BP and ending around 3360 cal. BP;

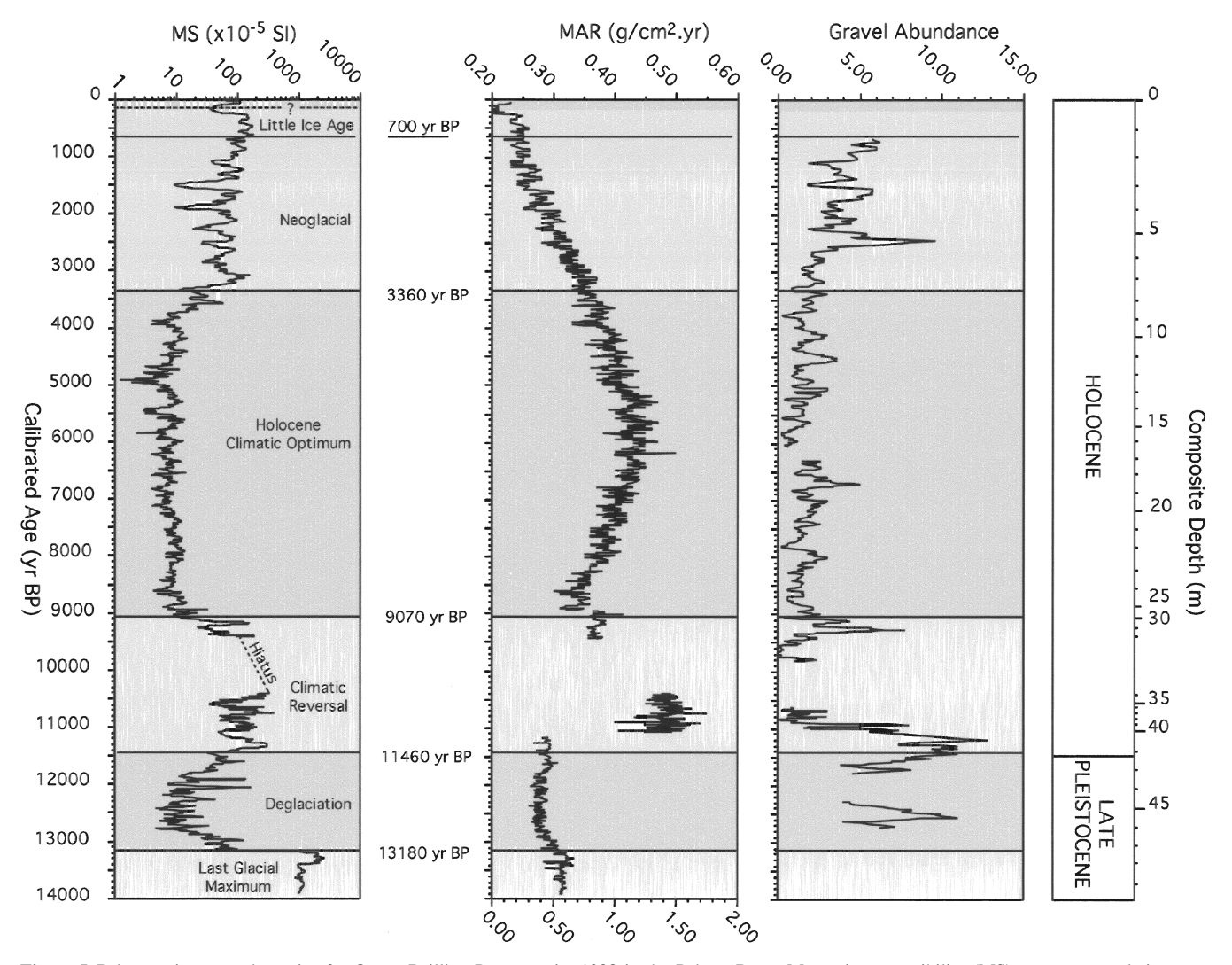


Figure 5 Palaeoenvironmental proxies for Ocean Drilling Program site 1098 in the Palmer Deep. Magnetic susceptibility (MS), mass accumulation rate (MAR g/cm².yr) and ice-rafted debris concentration (in gravel grains/5 cm core interval, following the standard methods of Grobe, 1987) are plotted versus calendar years and composite depth in the cores. Mass accumulation is determined using bulk density and the inverse of the first derivative of equation 1 and the linear sedimentation rates in Figure 2. For MAR, the 0.0–0.6 g/cm².yr scale is used for the 0–9000 cal. BP time period, and the 0.0–2.0 g/cm².yr scale for the 9000–14000 cal. BP time period.

- (3) a climatic cooling (reversal) beginning at 11460 cal. BP and ending abruptly at 9070 cal. BP;
- (4) an immediate deglacial episode of high primary production and iceberg rafting, from 13180 cal. BP to 11460 cal. BP; and
- (5) the Last Glacial Maximum (LGM) diamicton, deposited prior to 13180 cal. BP.

Neoglacial conditions are typified by greater concentrations of IRD, decreasing sediment accumulation and high MS (decreased productivity). The timing of Neoglacial onset agrees with most marine (Smith *et al.*, 1999) and terrestrial (Ingólfsson *et al.*, 1998) palaeoenvironmental records from the Peninsula, although these were based upon uncalibrated radiocarbon ages. In the Palmer Deep, the 'Little Ice Age' appears to have begun around 700 cal. BP, roughly in concert with GISP2 (Domack and Mayewski, 1999), Siple Dome (Kreutz *et al.*, 1997) and South African records (Repinski *et al.*, 1999).

The mid-Holocene climatic optimum is a prolonged period of enhanced productivity marked by maximum biogenic sediment accumulation and MAR of greater than 0.35 g/cm².yr (Figure 5). Minimum IRD concentration is associated with decreasing MS between 7300 cal. BP and 4700 cal. BP, coincident with climatic optimum conditions recognized in the Peninsula region (Ingólfsson *et al.*, 1998; Smith *et al.*, 1999). Global records are less coherent during this period, but in general the Palmer Deep

record correlates with the Boreal, Atlantic and Subboreal, all relatively warm chronozones of the European Holocene.

Spectral analyses of periodicity

For the Holocene portion of the record, spectral analysis of the MS data was completed using standard methods (Figure 6). Since the dynamic range of MS changes so dramatically around 3750 cal. BP, the data were divided into two sections: 0–3750 cal. BP (Figure 6A), and 3750–8950 cal. BP (Figure 6B).

For 0–3750 cal. BP, very significant peaks (above the 99% confidence level) occur at 400, 190, 122, 85 and 70 years. For 3750–8950 cal. BP, peaks at 400, 66, 52 and 40–42 years are above the 99% confidence level, and peaks at 190 and ~120 years are above the 90% confidence level. Previous application of spectral analysis on marine records from the Peninsula yielded a dominant period of 230 years (Palmer Deep) (Kirby *et al.*, 1998) and 278 years (Andvord Bay) (Domack *et al.*, 1993). However, given the improved chronological control presented here, we are more confident with our results. The ~200-year cyclicity remains strong throughout the Palmer Deep record and is also demonstrated by secular ¹⁴C fluctuations recorded in tree-rings (Suess and Linick, 1990; Stuiver and Braziunas, 1993) and in numerous other palaeoclimatic data sets as summarized previously (Kirby *et al.*, 1998). Although common periods do not necessitate a cause-and-effect

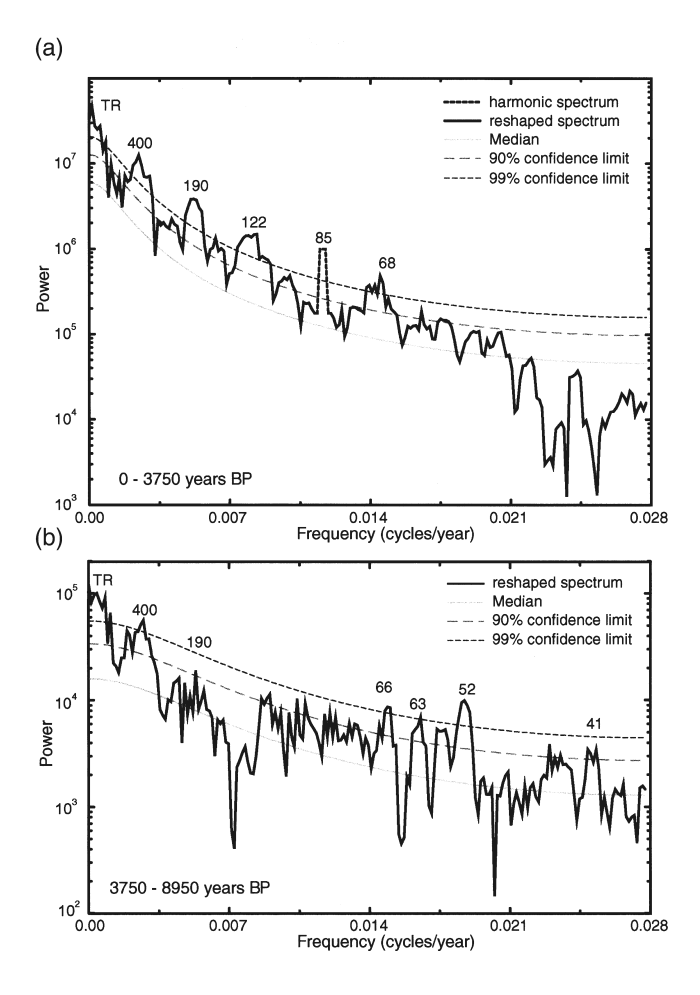


Figure 6 Multi-taper method spectral power plots of the magnetic susceptibility (MS) record from site 1098 for (A) 0–3750 cal. BP and (B) 3750–8950 cal. BP. The chronology for the MS data was assigned using the age model provided in equation (1). We used a sample spacing of seven years and three tapers. Numbers above the reshaped and harmonic spectra are the periods of the most specific spectral peaks, all of which rise above the 90% or 99% confidence limit. Significant power occurs at periods of about 400 and 190 years throughout the last 9000 years.

relationship, the predominance of so many records that demonstrate pronounced multicentury and decadal-scale cyclicity suggests a common forcing factor during the Holocene epoch (National Research Council, 1998), perhaps solar variability (Lean and Rind, 1998).

The multidecade cycles (those particularly in the 50-year range) may be related to oscillations in the Circum-Antarctic Trough (a zonal low-pressure system; Smith *et al.*, 1999) that is known to have variations at this same frequency in other portions of the Southern Ocean (Cook *et al.*, 1992). Although not addressed in this paper, spectral analysis of the entire Holocene portion of the grain-size record (a record that matches the MAR curve in Figure 5) of site 1098 demonstrates very significant variance at time period of 1800 years (Warner, 2000), thus demonstrating the preservation of millennial frequencies as well in this remarkable stratigraphic record.

Late-Pleistocene events

The climatic reversal and preceding deglacial episode are distinctive and allow us to define the Pleistocene to Holocene transition at a calendar age of 11460 cal. BP. This is in good agreement with the onset of the Holocene from European and North American records (Roberts, 1998). However, the chronology is far less constrained during this transition (Figure 3) than for the main Holocene and there are discrepancies with the timing of this event

compared to ice-core and other marine radiocarbon records (Stuiver et al., 1998). The climate reversal and preceding deglacial episode are quite similar in pattern and succession to the well-known Bølling/Allerød (B/A) to Younger Dryas (YD), but the transitions are out of phase with North Atlantic events and those documented recently from the Taylor Dome ice core (Mayewski et al., 1996; Steig et al., 1998). The climatic reversal in the Palmer Deep is marked by intensified ice rafting and reduced productivity, compatible with readvancing glacial fronts and iceberg concentrations along the periphery of the basin. Yet this event lags the classic YD episode by about 1000 calendar years and is considerably longer in duration, if the PD chronology is accurate over this time interval.

The deglacial episode is marked by enhanced productivity and reduced glacial influence within the basin, all preserved within a draped stratigraphic sequence above till (Figure 3). While there are hiatuses in the record, due to post-depositional erosion by gravity flows, there is sufficient section to determine that the deglacial period ranges from 13180 to 11460 cal. BP. That is roughly some 1000 calendar years after the B/A interval recorded in Greenland and Taylor Dome (Mayewski *et al.*, 1996; Steig *et al.*, 1998). Note, however, that there is a 500 to 1000-year variation in the precision of the Taylor Dome ice-core chronology over this same time interval (Steig *et al.*, 1998).

Deglaciation of the Palmer Deep is recorded by the transition from glacial diamicton (till) to laminated and varved diatom ooze/mud. Our age estimate of 13180 cal. BP for this event is several thousand years older than similar deglacial events from the Ross Sea (Domack et al., 1999; Cunningham et al., 1999) and Prydz Bay (O'Brien and Harris, 1996; Domack et al., 1998). Yet calibrated ages for the Ross Sea and Prydz Bay chronologies have yet to be presented. Globally, the deglacial event is in-phase with a time of decreased sea-level rise, associated with the YD (Fairbanks, 1989). While widespread glaciation of the Antarctic Peninsula shelf during the LGM has been an accepted assumption for some time (Pope and Anderson, 1992; Pudsey et al., 1994), the Palmer Deep data suggest a slightly earlier phase of deglaciation than proposed previously (Pudsey et al., 1994). Alternatively, there may have been less widespread glacial advance over the continental shelf during the stage-2 lowstand (Rebesco et al., 1998), keeping with other regional models for glaciation across the continental shelves of the Antarctic during the LGM (Domack et al., 1998; Shipp et al., 1999). Resolution of this problem awaits an independent chronology data base for sequences in and around the Palmer Deep region.

Conclusions

The application of radiocarbon dating methods (AMS) to the Palmer Deep sedimentary record has produced a high-resolution chronology consistent with global events during most of the Holocene. While some of these events, such as the 'Little Ice Age' and Neoglacial, appear in the Palmer Deep record some time earlier than in the Northern Hemisphere, others, such as the deglaciation and climatic reversal (potentially equivalent to the B/A and YD), occur later in the Palmer Deep record. Discrepancies in the timing of deglacial and subsequent climatic reversals could imply one of two scenarios. Either circum-Antarctic events during this period of climate instability are out of phase with those of the Northern Hemisphere, as opposed to the Taylor Dome ice-core results, or chronological constraints are still not good enough to resolve the exact timing of these events both in the Palmer Deep and Taylor Dome time-series. We favour the latter of the two working hypotheses and suggest a redoubling of efforts to obtain coordinated marine and ice-core chronologies from key areas of the circum-Antarctic, particularly from the region bordering the

Pacific sector of the Southern Ocean. The persistence and refinement of multicentury (~200-yr) scale periodicity in the record corroborate previous suggestions (Leventer et al., 1996) that solar modulation of the climate may be a characteristic of the Antarctic Peninsula region during the Holocene.

Acknowledgements

This work is supported by the Joint Oceanographic Institutions (JOI/USSSP funding for Ocean Drilling Program Leg 178) and the National Science Foundation, Office for Polar Programs (OPP-9615053 to Hamilton College, OPP-9714371 to Colgate University, OPP-9615695 to University of Minnesota and OPP-9615668 to Stanford University). The authors wish to thank Charles Borton for laboratory assistance. We are grateful for the timely support of our work at the University of Arizona NSF Accelerator Laboratory and for the additional analyses provided by Tom Guilderson via the Lawrence Livermore Laboratory.

References

Acton G., Borton, C. and Leg 178 Scientific Party 2000: Palmer Deep composite depth scales for ODP Leg 178 Sites 1098 and 1099, ODP Leg 178 Scientific Results, in press.

Andrews, J.T., Domack, E.W., Cunningham, W.L., Leventer, A., Licht, K.J., Jull, A.J.T., DeMaster, D.J. and Jennings, A.E. 1999: Problems and possible solutions concerning radiocarbon dating of surface marine sediments, Ross Sea, Antarctica. Quaternary Research 52(2), 20-216. Barker, P.F., Camerlenghi, A. and Acton, G. 1999: Proceedings of the Ocean Drilling Program, Initial Reports 178. Ocean Drilling Program, College Station, Texas.

Berkman, P.A. and Forman, S.L. 1996: Pre-bomb radiocarbon and the reservoir correction for calcareous marine species in the Southern Ocean. Geophysical Research Letters 23, 363-66.

Broecker, W.S., Sutherland, S. and Peng, T-H. 1999: A possible 20thcentury slowdown of Southern Ocean deep water formation. Science 286, 1132-35.

Cook, E.R., Bird, T., Peterson, M., Barbetti, M., Buckley, B.M., D'Arrigo, R. and Francey, R., 1992: Climatic change over the last millennium in Tasmania reconstructed from tree-rings. The Holocene 2, 205-17.

Cunningham, W.L., Leventer, A., Andrews, J.T., Jennings, A.E. and Licht, K.J. 1999: Late Pleistocene-Holocene marine conditions in the Ross Sea, Antarctica: evidence from the diatom record. The Holocene 9, 129 - 39

Domack, E.W. 1992: 14C ages and reservoir corrections for the Antarctic Peninsula and Gerlache Strait area. Antarctic Journal of the United States

Domack, E.W. and McClennen, C.E. 1996: Accumulation of glacial marine sediments in fjords of the Antarctic Peninsula and their use as late Holocene paleoenvironmental indicators. In Ross, R., Hoffman, E. and Ouetin, L., editors, Foundations for ecosystem research west of the Antarctic Peninsula, Washington DC: American Geophysical Union, 135-54. Domack, E.W. and Mayewski, P.A. 1999: Bi-polar ocean linkages: evidence from late-Holocence and Greenland ice-core records. The Holocene 9, 247-51.

Domack, E.W. and Reynolds, P. 1999: Cruise 98-2: Laurence M. Gould geology and geophysics report. Antarctic Journal of the United States 34, in press.

Domack, E.W., Jacobson, E.A., Shipp, S. and Anderson, J.B. 1999: Sedimentologic and stratigraphic signature of the Late Pleistocene/Holocene fluctuation of the West Antarctic Ice Sheet in the Ross Sea: a new perspective part 2. GSA Bulletin 111(10), 1517-36.

Domack, E.W., Mashiotta, T.A., Burkley, L.A. and Ishman, S.E. 1993: 300 year cyclicity in organic matter preservation in Antarctic fjord sediments. Antarctic Research Series 60, 265-72.

Domack, E.W., O'Brien, P., Harris, P., Taylor, F., Quilty, P., DeSantis, L. and Raker, B. 1998: Late Quaternary sediment facies in Prydz Bay, East Antarctica and their relationship to glacial advance onto the continental shelf. Antarctic Science 10, 236-46.

Fairbanks, R.G. 1989: A 17,000 year glacio-eustatic sea level record: influence of glacial melting rates on the Younger Dryas event and deep sea ocean circulation. Nature 342, 937-48.

Gordon, J.E. and Harkness, D.D. 1992: Magnitude and geographic variation of the radiocarbon content in Antarctic marine life; implications for reservoir correction in radiocarbon dating. Quaternary Science Reviews 11, 697–708.

Grobe, H. 1987: A simple method for the determination of ice-rafted debris in sediment cores. Polarforschung 57, 123-26.

Hughen, K.A., Overpeck, J.T., Lehman, S.J., Kashgarian, M., Southon, J., Peterson, L.C., Alley, R. and Sigman, D.M. 1998: Deglacial changes in ocean circulation from an extended radiocarbon calibration. Nature 391, 65-68.

Indermulhel, A., Stocker, T.F., Joos, F., Fischer, H., Smith, H.J., Wahlen, M., Deck, B., Mastroianni, D., Tschumi, J., Blunier, T., Meyer, R. and Stauffer, B. 1999: Holocene carbon-cycle dynamics based on CO2 trapped in ice at Taylor Dome, Antarctica. Nature 398, 121-26. Ingólfsson, Ó., Hjort, C., Berkman, P.A., Björk, S., Colhoun, E., Goodwin, I.D., Hall, B., Hirakawa, K., Melles, M., Möller, P. and Prentice, M.L. 1998: Antarctic glacial history since the last glacial maximum: an overview of the record on land. Antarctic Science 10, 326-44.

Katz, D. 2000: A rapid method for diatom analyses. Leg 178 Scientific Results, vol. 178, College Station Texas, in press.

Kirby, M.E., Domack, E.W. and McClennen, C.E. 1998: Magnetic stratigraphy and sedimentology of Holocene glacial marine deposits in the Palmer Deep, Bellingshausen Sea, Antarctica: implications for climate change? Marine Geology 152, 247-59.

Kreutz, K.J., Mayewski, P.A., Meeker, L.D., Twickler, M.S., Whitlow, S.I. and Pittalwala, I.I. 1997: I. Bipolar changes in Atmospheric circulation during the Little Ice Age. Science 277, 1294-96.

Lean, J. and Rind, D. 1998: Climate forcing by changing solar radiation. Journal of Climate 11, 3060-94.

Leventer, A. 1998: Varves from the Palmer Deep, Antarctica. Abstracts, American Geophysical Union Fall Meeting, San Francisco, California.

Leventer, A.R., Domack, E.W., Ishman, S.E., Brachfeld, S., McClennen, C.E. and Manley, P. 1996: Productivity cycles of 200–300 years in the Antarctic Peninsula region: understanding linkages among the sun, atmosphere, oceans, sea ice, and biota. GSA Bulletin 108, 1626-44.

Mayewski, P.A., Twickler, M.S., Whitlow, S.I, Meeker, L.D., Yang, Q., Thomas, J., Kreutz, K., Grootes, P.M., Morse, D.L., Steig, E.J., Waddington, E.D., Saltzman, E.S., Whung, P.Y. and Taylor, K.C. 1996: Climate change during the last deglaciation in Antarctica. Science 272, 1636-38.

McAndrews, E., Leventer, A. and Domack, E. 2000: Annual cycles in Palmer Deep Sediments. Antarctic Journal of the United States 34, in press.

National Research Council (US) 1998: Decade-to-century scale climate variability change: a science strategy. Washington DC: National Academy Press.

O'Brien, P.E. and Harris, P.T. 1996: Patterns of glacial erosion and deposition in Prydz Bay and the past behavior of the Lambert Glacier. Papers and Proceedings of the Royal Society of Tasmania 130, 79-85.

Pope, P.G. and Anderson, J.B. 1992: Late Quaternary glacial history of the northern Antarctic Peninsula's western continental shelf: evidence from the marine record. Antarctic Research Series 57, 63-91.

Pudsey, C.J., Barker, P.J. and Larter, R.D. 1994: Ice sheet retreat from the Antarctic Peninsula continental shelf. Continental Shelf Research 14, 1647-75.

Rebesco, M., Camerlenghi, A., DeSantis, L., Domack, E.W. and Kirby, M. 1998: Seismic stratigraphy of Palmer Deep: a fault-bounded late Quaternary sediment trap on the inner continental shelf, Antarctic Peninsula margin. Marine Geology 151, 89-110.

Repinski, P., Holmgren, K., Lauritzen, S.E. and Lee-Thop, J.A. 1999: A late Holocene climate record from a stalagmite, Cold Air Cave, Northern Province, South Africa. Palaeogeography, Palaeoclimatology, Palaeoecology 149, 651-59.

Roberts, N. 1998: The Holocene: an environmental history. Oxford: Blackwell.

Shipp, S., Anderson, J.B. and Domack, E.W. 1999: High-resolution seismic signature of the Late Pleistocene fluctuation of the West Antarctic Ice Sheet system in Ross Sea: a new perspective, Part 1. GSA Bulletin 111(10), 1486-516.

Smith, R.C., Ainley, D., Baker, K., Domack, E., Emslie, S., Fraser, B., Kennett, J., Leventer, A., Mosley-Thompson, E., Stammerjohn, S. and Vernet, M. 1999: Marine ecosystem sensitivity to climate change. Bioscience 49, 393-404.

Steig, E.J., Brook, E.J., White, J.M.C., Sucher, C.M., Bender, M.L., Lehman, S.J., Morse, D.L., Waddington, E.D. and Clow, G.D. 1998: Synchronous climate changes in Antarctica and the North Atlantic. Science 282, 92-95.

Stuiver, M. and Braziunas, T.F. 1993: Sun, ocean, climate and atmosphere 14CO2: an evaluation of causal and spectral relationships. The Holocene 3, 289-305.

Stuiver, M., Reimer, P., Bard, B., Beck, J.W., Burr, G.S., Hughen, K.A., Kromer, B., McCormac, G., Van Der Plicht, J. and Spurk, M. 1998: INTCAL98 radiocarbon age calibration, 24,000-0 cal. BP. Radiocarbon 40, 1041-83.

Suess, M. and Linick, T.W. 1990: The ¹⁴C record in bristlecone pine of the past 8000 years based on the dendrochronology of the late C.W. Ferguson. Philosophical Transactions of the Royal Society of London A330, 403-12.

Thompson, L.G., Peel, D.A., Mosley-Thompson, E., Mulvaney, R., Dai, J., Lin, P.N., Davis, M.E. and Raymond, C.F. 1994: Climate since AD 1510 on the Dyer Plateau, Antarctic Peninsula: evidence for recent climate change. Annals of Glaciology 20, 420-26.

Warner, N.R. 2000: Grain size analysis in the Palmer Deep, Antarctica: high resolution paleoclimatic record of the Holocene SE Pacific, Bellingshausen Sea. BA thesis, Hamilton College, Clinton NY, 110 pp.